Laser frequency instability of 6×10^{-16} using 10-cm-long cavities on a cubic spacer

Xiaotong Chen (陈晓彤)[1], Yanyi Jiang (蒋燕义)[1,*], Bo Li (李 波)[1], Hongfu Yu (于洪浮)[1], Haifeng Jiang (姜海峰)[2], Tao Wang (王 涛)[3], Yuan Yao (姚 远)[1,], and Longsheng Ma (马龙生)[1]**

[1]*State Key Laboratory of Precision Spectroscopy, East China Normal University, Shanghai 200062, China*
[2]*Key Laboratory of Time and Frequency Primary Standards, National Time Service Center, Xi'an 710600, China*
[3]*AVIC Xi'an Flight Automatic Control Research Institute, Xi'an 710065, China*
**Corresponding author: yyjiang@phy.ecnu.edu.cn; **corresponding author: yyao@lps.ecnu.edu.cn*
Received September 18, 2019; accepted November 22, 2019; posted online February 21, 2020

We demonstrate two ultra-stable laser systems at 1064 nm by independently stabilizing two 10-cm-long Fabry–Pérot cavities. The reference cavities are on a cubic spacer, which is rigidly mounted for both low sensitivity to environmental vibration and ability for transportation. By comparing against an independent ultra-stable laser at 578 nm via an optical frequency comb, the 1064 nm lasers are measured to have frequency instabilities of 6×10^{-16} at 1 s averaging time.

Keywords: laser stabilization; Fabry-Pérot cavity; linewidth.
doi: 10.3788/COL202018.030201.

Lasers with high-frequency stability and narrow linewidth are indispensable tools in optical frequency standards, gravitational wave detection, low noise optical/microwave synthesis, and tests of fundamental physics[1–5]. While significant progress towards 10^{-17} laser frequency instability has been achieved[6–8], there is growing interest in transportable ultra-stable laser systems for many practical applications. In geodesy, to precisely measure the gravity potential difference at two sites, transportable optical atomic clocks are required to obtain the frequency difference at two sites in order to mitigate the risk of undetected errors[9]. Thus, ultra-stable laser systems as local oscillators in optical atomic clocks are required to be transportable[10,11]. For applications in space, such as the Gravity Recovery and Climate Experiment Follow-On (GRACE-FO) and gravitational wave detection[12–14], laser interferometry is a sensitive way to measure relative distance change, where the measurement sensitivity relies on the laser frequency stability.

Lasers with high-frequency stability are usually achieved by locking the laser frequency to the resonance of ultra-stable Fabry–Pérot (FP) cavities with the Pound–Drever–Hall (PDH) technique[15]. The laser frequency stability relies mostly on the length stability of the reference cavity. Efforts have been paid in the last decade to construct reference cavities with low vibration sensitivities of $10^{-11}/g$ to $10^{-10}/g$[16–18].

One of the most critical parts concerning transportability is the support of reference cavities, since cavities usually rest under their weight and remain in a fixed orientation with respect to gravity. To solve this problem, reference cavities should be constrained in all degrees of freedom. Moreover, they might be better to be symmetrically held at special positions for low vibration sensitivity. In 2011, a spherical cavity with a diameter of 5 cm was rigidly supported at two points on a diameter of the sphere at a squeeze-insensitive angle with respect to the optical axis[19]. Acceleration sensitivities of the reference cavity along three directions below $3 \times 10^{-10}/g$ and a laser frequency instability of 1×10^{-15} at 1 s averaging time were achieved. In the same year, Webster *et al.* constructed a 5-cm-long cubic cavity with four supports placed symmetrically about the optical axis in a tetrahedral configuration[20]. An acceleration sensitivity better than $2.5 \times 10^{-11}/g$ was achieved. In 2012, Argence *et al.* reported a 10-cm-long cylinder cavity rigidly held at its mid-plane[21]. Acceleration sensitivities of the reference cavity along three directions below $4 \times 10^{-10}/g$ and a laser frequency instability of 6×10^{-16} at 1 s were achieved. Using a similar cavity, Tai *et al.* obtained a sub-hertz linewidth 1555 nm laser with a frequency instability of 7×10^{-16} at 1 s[22]. In 2014, Chen *et al.* constructed a 10-cm-long cylinder cavity rigidly held at 10 pairs of points on the cavity spacer[23]. Acceleration sensitivities of the cavity along three directions below $4 \times 10^{-10}/g$ and a laser frequency instability of 1×10^{-15} at 1 s averaging time were achieved. Later, a laser frequency instability of 4×10^{-16} at 10 s averaging time was obtained by locking to a 12-cm-long cavity with a similar structure. In 2018, a similar 10-cm-long cuboid cavity was mounted rigidly and tested by dropping from a height of 25 cm, corresponding to an acceleration of $100g$[24].

In this Letter, two 10-cm-long optical cavities based on a cubic spacer are constructed. The cavity spacer is supported at four points in a tetrahedral arrangement, similar to the 5-cm-long cavity in Ref. [20]. However, we realize two optical cavities on the same cavity spacer. The sensitivities of the cavity length to accelerations along three directions are measured to be $(0.9–2) \times 10^{-10}/g$. Two 1064 nm neodymium-doped yttrium aluminum garnet

(Nd:YAG) lasers are separately frequency-stabilized to the resonance of the reference cavities. By comparing against an independent 578 nm laser with better frequency stability via an optical frequency comb, each transportable 1064 nm laser is measured to have a frequency instability of $\sim 6 \times 10^{-16}$ at 1 s averaging time. With additional measurement between two 1064 nm lasers stabilized to two cavities based on a single cubic spacer, we deduce that vibration noise is partially correlated to both optical cavities.

To achieve a cavity thermal noise-limited laser frequency instability at the 10^{-16} level, the cavity length is chosen to be 100 mm, and two fused silica (FS) mirrors with lower mechanical loss, compared to that of ultralow-expansion (ULE) glass, are optically contacted onto the cavity ends. According to Refs. [25] and [26], the cavity thermal noise-limited laser frequency instability and laser frequency noise at the Fourier frequency of 1 Hz are estimated to be 4.3×10^{-16} and 0.09 Hz/$\sqrt{\text{Hz}}$, respectively. For the cavity thermal noise-limited laser frequency noise at Fourier frequency of 1 Hz, the Brownian motion of the mirror coating and substrate, and the coating thermoelastic noise contribute 73%, 11%, and 15% over all the cavity thermal noise, respectively.

In order to make the reference cavities insensitive to vibration, here the geometry of the cavity spacer is designed to be as symmetrical as possible. As shown in Fig. 1(a), the cavity spacer is a cubic geometry with a side length of 100 mm. Along each axis, there is a hole with a diameter of 10 mm passing through the center of the cubic spacer for optical access or evacuation. Two pairs of highly-reflective FS mirrors are optically contacted to the cubic spacer in the horizontal plane (in the x–y plane). The optical axis of cavity 1 is along the x axis, while that of cavity 2 is along the y axis. For each pair of mirrors, one is a plane, and the other one has a concave radius of curvature of 1 m. The finesse and reflection contrast of each cavity are ~700,000 and ~40%, respectively. At the backside of each mirror, a ULE glass ring is contacted to reduce the thermal expansion of the FS mirror. For convenient supporting, the vertices of the cubic spacer are truncated to a depth of 7.8 mm toward the center of the spacer. In each truncated face, there is a cone in the center. Four of the cones in a tetrahedral arrangement are used to locate Viton balls, which are squeezed toward the center of the cavity by screws, as shown in Fig. 1(b).

Based on numerical analysis, the fractional change of the cavity length under a compressive force of 1 N applied at each support is on the order of 10^{-11} when the cut depth is changed from 0 mm to 17.3 mm. This deformation is much smaller than the tolerance of machining (0.1 mm). For this reason, we choose the cutting depth only for convenient supporting.

Due to symmetrical geometry, the cavity length is insensitive to acceleration if the light spots are in the center of mirrors, as shown in Fig. 1(c), based on numerical analysis, where an acceleration of $1g$ is applied along the air hole (the z axis). The sensitivities of two cavities

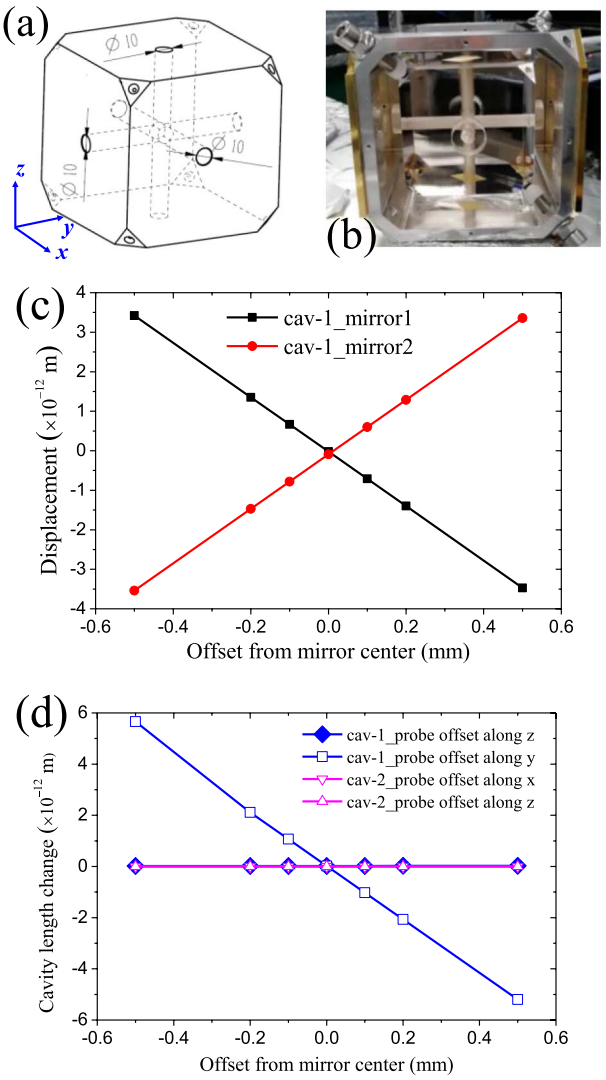

Fig. 1. Design of transportable reference cavities. (a) The cubic cavity spacer. (b) The cavities mounted on an aluminum cage. (c) The displacement of probe points at different positions along the z axis on the mirrors of cavity 1 under an acceleration of $1g$ along the z axis. (d) The length change of two cavities under an acceleration of $1g$ along the y axis. Three curves are overlapped.

to vertical vibration depend on the light spots on the mirrors. If the light spots are 0.5 mm offset from the mirror center along the z axis, the vibration sensitivity of each cavity will be $7 \times 10^{-11}/g$, which does not change by 30% when the cutting depth changes from 0 mm to 17.3 mm. Under the acceleration along the z axis, the length change of two cavities is similar, which indicates that vibration noise along the z axis may be common to both cavities to some extent, depending on the offset of light spots from the center of the mirrors.

When acceleration is applied in the horizontal plane, e.g., along the y axis, the cavity length change is shown in Fig. 1(d). The length of cavity 2 is insensitive to it, since both mirrors are displaced by the same mount, while the length of cavity 1 changes depending on the offset of light spots from the mirror centers. It indicates that in this case

the vibration sensitivities of two cavities might not be common. When vibration is not along the cavity optical axis, it is common to both cavities to a certain extent, depending on the angle of vibration with respect to the cavity optical axes. For example, when acceleration is applied at 45° with respect to the cavity optical axes, the vibration sensitivities of two cavities may be common. Assuming vibration is distributed uniformly in the x–y plane, half of the vibration noise is common to both cavities.

Experimentally, the optical cavities are rigidly supported in an aluminum cage covered by gold-plated copper plates to reflect thermal radiation, which behave as thermal low-pass filters. We keep the forces of mounting the cavity on the four supporting points constant in order to support the cavity as symmetrically as possible. Then, the cage is enclosed in another thermal shield made of gold-plated copper as a second-order thermal low-pass filter. Outside, there is a vacuum chamber evacuated to 5×10^{-8} Torr (1 Torr = 133.32 Pa) to reduce the fluctuation of the index of refraction and the convective heat flow through air. The temperature of the vacuum chamber is stabilized at about 27°C with a fluctuation within 2 mK in order to make the temperature of the optical cavities stable. The response time of the cavities to the temperature change of the vacuum chamber is measured to be 58 h. Moreover, the vacuum chamber, as well as the optics for PDH detection, is placed in a home-made acoustic isolation box. The box is installed with four wheels underneath for easy transportation.

Two Nd:YAG lasers at 1064 nm with a free running linewidth of ~1 kHz are separately frequency-stabilized to the resonance of the cubic cavities. For each laser, the laser light is split into several parts. When using optical polarization maintaining (PM) fibers to transfer the light to the reference cavities, fiber noise cancellation (FNC)[27] is employed to remove random phase/frequency noise induced by the optical fibers, as shown in Fig. 2(b).

On the platform of the reference cavity, as shown in Fig. 2(a), the laser light transferred through the PM fiber is frequency-shifted by an acousto-optic modulator (AOM). The first-order diffraction efficiency of the AOM is adjusted for light power stabilization by controlling the power of the driving radio frequency (RF) signal according to a dc signal monitored on a photo-detector (PD_1) before the reference cavity. Then, the diffraction laser light from the AOM passes through a polarizer (P_1), and it is phase-modulated at about 4 MHz in an electro-optic modulator (EOM). An optical isolator (Iso) is placed after the EOM to prevent any light reflected back into the EOM for the reduction of the residual amplitude modulation (RAM). After phase modulation, the light is coupled to its reference cavity. The cavity reflection light is steered onto PD_2, which is resonant at the modulation frequency of the EOM. Then, the detected RF signal is demodulated to generate a PDH-based frequency discrimination signal for laser frequency stabilization. The PDH signal is fed back to a piezo inside the laser cavity to control the laser frequency. The laser servo bandwidth is about 50–80 kHz.

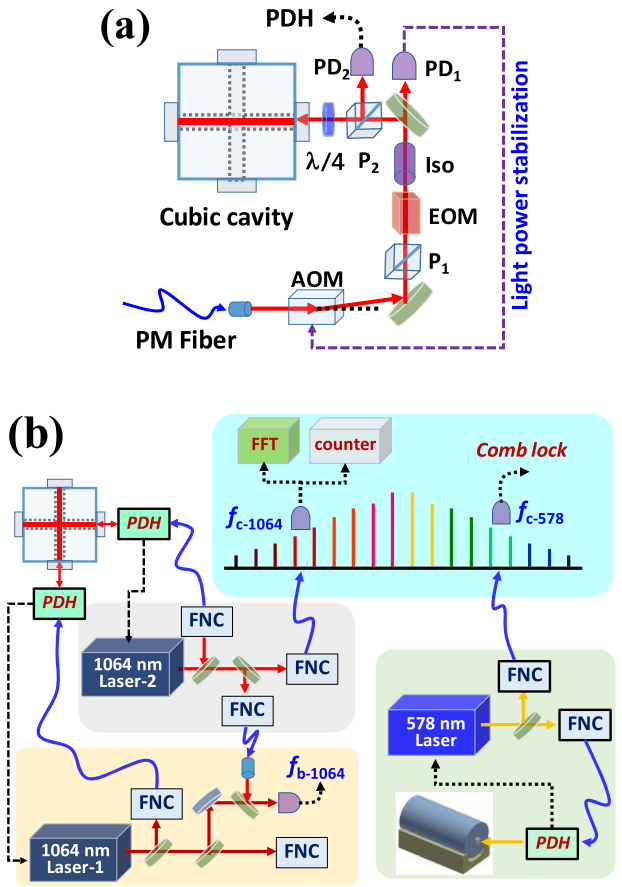

Fig. 2. Schematic diagram of the experimental setup for (a) laser frequency stabilization and (b) laser performance measurement. AOM, acousto-optic modulator; FNC, fiber noise cancellation; P, polarizer; EOM, electro-optic modulator; Iso, optical isolator; $\lambda/4$, quarter-wave plate; PD, photo-detector; FFT, fast Fourier transform spectrum analyzer.

While the cavity is designed for transportability, another primary challenge to achieve laser frequency instability below 10^{-15} is that the cavity length should also be insensitive to vibration noise. We denote S_i ($i = x, y, z$) as the sensitivity of the cavity length to vibration along the x, y, or z axis, $S_i = \Delta L/(L \times a_{v-i})$, where L is the cavity length, and ΔL is the cavity length change only due to an acceleration a_{v-i}. To measure the vibration sensitivity, the laser light from a third independent cavity-stabilized laser at 1064 nm was transferred to the platform of the cubic cavities. The schematic diagram for measuring the cavity vibration sensitivity is similar to that described in Ref. [28]. Each time we purposely applied shake with power spectral density (PSD) of $10^{-3} g/\sqrt{\text{Hz}}$ accordingly along one of the x, y, and z axes to an active vibration isolation platform where the cubic cavity was. When light was resonant on the cubic cavity, the PDH-based frequency discrimination signal from the cubic cavity was measured on a fast Fourier transform (FFT) spectrum

analyzer. The PSD of the PDH signal at the shaking frequency was then scaled to laser frequency noise ν_{vib} with the slope of the PDH signal. Meanwhile, an accelerometer measured the acceleration a_{v-i} at the shaking frequency along $i = x$, y, and z. Actually, the laser frequency noise ν_{vib} is induced by the accelerations along all three axes. Therefore, $\nu_{\mathrm{vib}} = [(S_x \times a_{v-x} \times \nu_0)^2 + (S_y \times a_{v-y} \times \nu_0)^2 + (S_z \times a_{v-z} \times \nu_0)^2]^{0.5}$, where ν_0 is laser frequency. With three equations obtained from three measurements (in each measurement, an acceleration was applied to one of the x, y, and z axes), we can deduce the sensitivity of the cavity length to vibration along the z axis S_z to be $2 \times 10^{-10}/g$ and the sensitivities of the cavity length to vibration along and perpendicular to the cavity optical axis to be $9 \times 10^{-11}/g$ and $2 \times 10^{-10}/g$, respectively. The measured vibration sensitivities are larger than the simulation results, which may arise from the offset of the light spot from the mirror center, the offset of the mirror center from the center of the spacer, or unbalanced supporting of the spacer. In normal operation, the cubic cavities are placed on a passive vibration isolation platform. When the vibration isolation platform is activated, the PSD of the acceleration on the platform at a Fourier frequency of 1 Hz is about $1 \times 10^{-6} g/\sqrt{\mathrm{Hz}}$. Thus, we evaluate the total vibration-induced laser frequency noise at 1 Hz to be $0.08\,\mathrm{Hz}/\sqrt{\mathrm{Hz}}$, about the same as that induced by the cavity thermal noise.

Besides vibration, other significant contributions such as the light power instability and RAM are evaluated. The power instabilities of the light incident into the cavities are 2×10^{-5} at 1 s averaging time. Since the sensitivity of the cavity length to the change of incident light power is about $25\,\mathrm{Hz}/\mu\mathrm{W}$ at input light power of $10\,\mu\mathrm{W}$, the light power instability-induced cavity length fluctuation is evaluated to be 2×10^{-17} at 1 s averaging time. To measure the contribution from RAM, the PDH-based frequency discrimination signals, when the light is off resonant, are monitored on a high-precision multimeter. Those signals are then converted to laser frequency fluctuation with the slope of the PDH signal. It shows that RAM-induced laser frequency instabilities for both cavities are 1×10^{-16} at 1 s averaging time.

Based on the above analysis, we learn that vibration and thermal noise contribute mostly to the laser frequency noise. The thermal noise from two cavities on the same cubic spacer is not correlated, while vibration noise is partially common to both cavities based on numerical analysis. The maximum correlation happens when vertical vibration is fully common to both cavities and half of horizontal vibration is common to both cavities. In this case, the frequency instability of the beat note between two frequency-stabilized 1064 nm lasers is $\sqrt{3}$ times less than that measured between independent cavity-stabilized lasers. When vertical vibration is uncorrelated to both cavities, the frequency instability between two frequency-stabilized 1064 nm lasers is only $\sqrt{(3/2)}$ times less than an independent measurement.

Here, we evaluate the performance of two frequency-stabilized 1064 nm lasers and the correlation between them by measuring the frequency instabilities among two frequency-stabilized 1064 nm lasers and an independent cavity-stabilized 578 nm laser with better frequency stability[26]. To cover the wide spectral range between those lasers, an optical frequency comb is employed[29,30]. The comb light is generated from a Ti:sapphire femtosecond laser, and its spectrum is broadened in a photonics crystal fiber, similar to that reported in Ref. [31]. The carrier-envelope offset frequency of the comb is detected with the collinear self-referencing 1f–2f technique, and it is phase-locked to an RF synthesizer.

Figure 2(b) shows the experimental diagram. A portion of the 1064 nm laser 2 is transferred to the 1064 nm laser 1 through a piece of PM fiber to generate a beat note $f_{b\text{-}1064}$ between two 1064 nm lasers. The light from the 578 nm laser is transferred to the platform where the comb is. The beat note $f_{c\text{-}578}$ between the 578 nm laser light and its nearby comb tooth is detected and used to control the comb repetition rate by adjusting the length of the Ti:sapphire laser cavity. After being stabilized, each comb tooth has a performance similar to the 578 nm laser.

The frequency of the beat note $f_{c\text{-}1064}$ between one of the 1064 nm lasers and its nearby comb tooth was recorded on a counter with a gate time of 1 s. The fractional frequency instabilities of the beat notes are shown in Fig. 3 with blue triangles (578 nm versus 1064 nm laser 1) and red diamonds (578 nm versus 1064 nm laser 2). Since the 578 nm laser has a frequency instability of 3.5×10^{-16} at 1 s averaging time, we can deduce that the frequency instabilities of two 1064 nm lasers are $\sigma_1 = 5.6 \times 10^{-16}$ and $\sigma_2 = 6.8 \times 10^{-16}$ at 1 s averaging time. The frequency instability of f_{b-1064} (black circles) is measured to be 7.4×10^{-16} at 1 s averaging time. It is nearly $\sqrt{(3/2)}$ times less than that independently measured against the 578 nm laser, $(\sigma_1^2 + \sigma_2^2)^{1/2} = 8.8 \times 10^{-16}$. This indicates vibration along the z axis may be partially uncommon to the 1064 nm cavities on the same cubic spacer.

In conclusion, two 1064 nm lasers with frequency instabilities of 5.6×10^{-16} and 6.8×10^{-16} at 1 s averaging time are demonstrated. Both the cavity thermal noise and

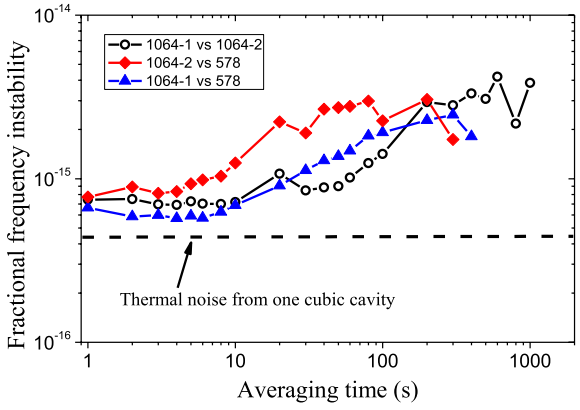

Fig. 3. Laser frequency instability measurement.

vibration contribute equally to the laser frequency noise. Vertical vibration noise may be partially uncommon to the two 1064 nm cavities on the same cubic spacer. The frequency-stabilized lasers to the cubic FP cavities have been transported to another room over 300 m at the same building. After transportation, we connected all the electronics and relocked the laser frequencies to the cavities without optical alignment. In the next step, the supporting of the cubic cavities will be modified to achieve an even lower vibration sensitivity and better frequency stability. Those laser systems will also be transported to other cities for the measurement of the frequency ratios between optical atomic clocks and applications in gravitational wave detection.

This work was supported by the National Natural Science Foundation of China (Nos. 11654004, 11822402, 91636214, and 11804094) and the National Key R&D Program of China (No. 2017YFA0304403).

References

1. A. D. Ludlow, M. M. Boyd, J. Ye, E. Peik, and P. O. Schmidt, Rev. Mod. Phys. **87**, 637 (2015).
2. Y. Li, Y. Lin, Q. Wang, T. Yang, Z. Sun, E. Zang, and Z. Fang, Chin. Opt. Lett. **16**, 051402 (2018).
3. B. Willke, K. Danzmann, M. Frede, P. King, D. Kracht, P. Kwee, O. Puncken, R. L. Savage, B. Schulz, F. Serfert, C. Veltkamp, S. Wagner, P. Weβels, and L. Winkelmann, Class. Quantum Grav. **25**, 114040 (2008).
4. Y. Yao, Y. Jiang, L. Wu, H. Yu, Z. Bi, and L. Ma, Appl. Phys. Lett. **109**, 131102 (2016).
5. T. M. Fortier, M. S. Kirchner, F. Quinlan, J. Taylor, J. C. Bergquist, T. Rosenband, N. Lemke, A. Ludlow, Y. Jiang, C. W. Oates, and S. A. Diddams, Nat. Photon. **5**, 425 (2011).
6. D. G. Matei, T. Legero, S. Häfner, C. Grebing, R. Weyrich, W. Zhang, L. Sonderhouse, J. M. Robinson, J. Ye, F. Riehle, and U. Sterr, Phys. Rev. Lett. **118**, 263202 (2017).
7. W. Zhang, J. M. Robinson, L. Sonderhouse, E. Oelker, C. Benko, J. L. Hall, T. Legero, D. G. Matei, F. Riehle, U. Sterr, and J. Ye, Phys. Rev. Lett. **119**, 243601 (2017).
8. S. Häfner, S. Falke, C. Grebing, S. Vogt, T. Legero, M. Merimaa, Ch. Lisdat, and U. Sterr, Opt. Lett. **40**, 2112 (2015).
9. J. Grotti, S. Koller, S. Vogt, S. Häfner, U. Sterr, Ch. Lisdat, H. Denker, C. Voigt, L. Timmen, A. Rolland, F. N. Baynes, H. S. Margolis, M. Zampaolo, P. Thoumany, M. Pizzocaro, B. Rauf, F. Bregolin, A. Tampellini, P. Barbieri, M. Zucco, G. A. Costanzo, C. Clivati, F. Levi, and D. Calonico, Nat. Phys. **14**, 437 (2018).
10. S. B. Koller, J. Grotti, St. Vogt, A. Al-Masoudi, S. Dörscher, S. Häfner, U. Sterr, and Ch. Lisdat, Phys. Rev. Lett. **118**, 073601 (2017).
11. J. Cao, P. Zhang, J. Shang, K. Cui, J. Yuan, S. Chao, S. Wang, H. Shu, and X. Huang, Appl. Phys. B **118**, 073601 (2017).
12. B. S. Sheard, G. Heinzel, K. Danzmann, D. A. Shaddock, W. M. Klipstein, and W. M. Folkner, J. Geod. **86**, 1083 (2012).
13. R. X. Adhikari, Rev. Mod. Phys. **86**, 121 (2014).
14. J. Luo, L.-S. Chen, H.-Z. Duan, Y.-G. Gong, S. Hu, J. Ji, Q. Liu, J. Mei, V. Milyukov, M. Sazhin, C.-G. Shao, V. T. Toth, H.-B. Tu, Y. Wang, Y. Wang, H.-C. Yeh, M.-S. Zhan, Y. Zhang, Y. Zhang, V. Zharov, and Z.-B. Zhou, Class. Quant. Grav. **33**, 035010 (2016).
15. R. W. P. Drever, J. L. Hall, F. V. Kowalski, J. Hough, G. M. Ford, A. J. Munley, and H. Ward, Appl. Phys. B **31**, 97 (1983).
16. L. Chen, J. L. Hall, J. Ye, T. Yang, E. Zang, and T. Li, Phys. Rev. A **74**, 053801 (2006).
17. T. Nazarova, F. Riehle, and U. Sterr, Appl. Phys. B **83**, 531 (2006).
18. S. A. Webster, M. Oxborrow, and P. Gill, Phys. Rev. A **75**, 011801 (2007).
19. D. R. Leibrandt, M. J. Thorpe, M. Notcutt, R. E. Drullinger, T. Rosenband, and J. C. Bergquist, Opt. Express **19**, 3471 (2011).
20. S. Webster and P. Gill, Opt. Lett. **36**, 3572 (2011).
21. B. Argence, E. Prevost, T. Lévèque, R. Le Goff, S. Bize, P. Lemonde, and G. Santarelli, Opt. Express **20**, 25409 (2012).
22. Z.-Y. Tai, L.-L. Yan, Y.-Y. Zhang, X.-F. Zhang, W.-G. Guo, S.-G. Zhang, and H.-F. Jiang, Chin. Phys. Lett. **34**, 090602 (2017).
23. Q.-F. Chen, A. Nevsky, M. Cardace, S. Schiller, T. Legero, S. Häfner, A. Uhde, and U. Sterr, Rev. Sci. Instr. **85**, 113107 (2014).
24. B. K. Tao and Q. F. Chen, Appl. Phys. B **124**, 228 (2018).
25. K. Numata, A. Kemery, and J. Camp, Phys. Rev. Lett. **93**, 250602 (2004).
26. G. D. Cole, W. Zhang, M. J. Martin, J. Ye, and M. Aspelmeyer, Nat. Photon. **7**, 644 (2013).
27. L. S. Ma, P. Jungner, J. Ye, and J. L. Hall, Opt. Lett. **19**, 1777 (1994).
28. L. Jin, Y. Jiang, Y. Yao, H. Yu, Z. Bi, and L. Ma, Opt. Express **26**, 18699 (2018).
29. J. L. Hall, Rev. Mod. Phys. **78**, 1279 (2006).
30. T. W. Hansch, Rev. Mod. Phys. **78**, 1297 (2006).
31. Y. Jiang, Z. Bi, L. Robertsson, and L. Ma, Metrologia, **42**, 304 (2005).